

## Temperature effect on graphite KS44 lithiation in ethylene carbonate + propylene carbonate solution: galvanostatic and impedance study

B. BLIZANAC<sup>1,\*</sup>, S. MENTUS<sup>1</sup>, N. CVIJETIĆANIN<sup>1</sup> and N. PAVLOVIĆ<sup>2</sup>

<sup>1</sup>Faculty for Physical Chemistry, Studentski trg 12–16, Belgrade and <sup>2</sup>The Military Technical Institute of the Yugoslav Army, Katanićeva 15, Belgrade, Yugoslavia

(Received 18 August, revised 23 October 2002)

*Abstract:* Graphite Lonza KS44 in a solution 1 M LiClO<sub>4</sub> in a propylene carbonate + ethylene carbonate (1 M:1 M) mixture was lithiated and delithiated galvanostatically at room temperature and at the elevated temperature of 55 °C. Voltage–time profiles and complex impedance diagrams were recorded and are discussed for this particular system. It was confirmed that this type of graphite shows a relatively small current loss consumed by exfoliation, if lithiated at room temperature. However, the voltage–time curve of the first charging at 55 °C shows a long voltage plateau at 0.7 V vs. Li/Li<sup>+</sup>, which corresponds to 540 mAh g<sup>-1</sup> of irreversible capacity attributed to exfoliation. The solid electrolyte layer formed at elevated temperature, although less protecting in the sense of electrolyte reduction, shows a remarkably higher electrical resistance than that formed at room temperature. A comparison of the impedance diagrams of lithiated and delithiated samples allows the conclusion that mass transfer through the graphite, not that through the solid electrolyte layer, plays a dominant role in the mass transfer limitations.

*Keywords:* graphite, lithiation, reversible capacity, galvanostatic charging, solid electrolyte layer.

### INTRODUCTION

Lithiated graphite is now the generally accepted anode for lithium-ion batteries because of its high capacity (more than 300 mAh/g, for compositions close to LiC<sub>6</sub>), flat potential profile, and reasonable cost.<sup>1</sup> A typical lithium-ion cell is made up of a coke or graphite anode, an electrolyte soaked separator which serves as an ionic path between the electrodes and mechanically separates the two materials, and a lithiated metal oxide (such as LiCoO<sub>2</sub>, LiMn<sub>2</sub>O<sub>4</sub>, or LiNiO<sub>2</sub>) as the cathode. The successful operation of Li-ion cells is attributed mainly to surface films on the carbonaceous anode materials, which are formed in suitable electrolytes during the first charging, when a part of the intercalated

\* Corresponding author, current address: Materials Science Division, Lawrence Berkeley National Laboratory, University of California, Berkeley, CA 94720, USA; phone: ++1-510-486-4793, fax: ++1-510-486-5530, e-mail: BBBBlizanac@lbl.gov.

lithium reduces solvent molecules and is transformed mainly to lithium carbonate. The film formation starts when the potential of the graphite reaches a negative enough value, approx. 1 V vs. Li/Li<sup>+</sup>, and it covers the entire electrode surface exposed to the electrolyte. The surface film shows a moderate ionic conductivity and, hence, is termed a “solid electrolyte interface” (SEI). The charge consumed for SEI formation is called irreversible capacity, since this part of charge cannot be extracted during the discharging process.<sup>1</sup> This film, separating the electrolyte and the lithiated graphite, provides the much-needed kinetic stability to electrolyte species even at anode potentials where thermodynamically reduction may occur. The SEI permeability to Li<sup>+</sup> cations permits further graphite intercalation and deintercalation. Understandably, the performance of an anode is dictated largely by the characteristics of the SEI, *i.e.*, its resistance, ability to prevent further electrolyte reduction, amenability to charge transfer or the Li intercalation process and, to some extent, the diffusivity of Li<sup>+</sup> ions, even though it is difficult to distinguish the slow diffusion across the SEI from the slow diffusion process within the bulk anode. The corresponding performances characteristic of Li-ion cells that are affected by the SEI include: cycle life, self-discharge, rate capability and low working temperature.

The early attempts to synthesize lithium/graphite intercalation compounds by cathodic polarization of graphite in aprotic electrolytes based on polar solvents such as propylene carbonate (PC) containing Li-salt yielded ternary graphite intercalation compounds containing both lithium and solvent (Li<sub>x</sub>(solv)<sub>y</sub>C<sub>6</sub>) (the process is frequently called “solvated intercalation”).<sup>1,2</sup> In propylene carbonate, the formation of these solvated compounds is more favorable than the formation of the binary unsolvated compound Li<sub>x</sub>C<sub>6</sub> (the potential of which is more negative). Solvated intercalation is an undesirable appearance, since solvated intercalation compounds are thermodynamically and kinetically unstable due to the facile reduction of the cointercalated molecules. After the discovery that the products of ethylene carbonate (EC) reduction form a good protective SEI on external graphite surfaces,<sup>3–5</sup> EC based electrolytes are currently generally used to suppress solvated intercalation. Nevertheless, even in EC-based electrolytes, solvated lithium/graphite compounds participate to some extent in the first charging process, and their reduction leads to an additional irreversible charge loss, or irreversible capacity. These reactions can also take place on internal surfaces between the graphene layers<sup>4,6</sup> forming an “extra” film which penetrates into the bulk of the graphite host.<sup>3,4,7–9</sup>

Recently, new data on the performance of SEI on lithiated carbons, involving studies of the influence of temperature, have been obtained.<sup>5,10–16</sup> The cycle life of graphite was shown to be enlarged by pre-cycling at a lower temperature,<sup>5</sup> and the cycle life of a lithiated graphite anode was shown to be shortened remarkably when it was cycled at an elevated temperature.<sup>10,11</sup> MacNeil *et al.*<sup>12</sup> evidenced the difference in reactivity of various lithiated carbons against electrolyte at different temperatures. Zheng *et al.*<sup>13</sup> showed that prolonged storage at elevated temperatures reduces both the reversible capacity and the kinetics of electrochemical lithiation/delithiation of different types of lithiated Osaka Gas Co. graphites. Anderson *et al.*<sup>14</sup> outlined the considerable role of the nature of the lith-

ium salt on the composition of the SEI under heat treatment. Wang *et al.*,<sup>15</sup> and to some extent Aurbach *et al.*,<sup>16</sup> used the impedance method to study the formation kinetics and the nature of the surface films on different types of carbon at elevated temperatures, whereby they confirmed the results reported elsewhere<sup>10,11</sup> that temperature elevation shortens the cycle life of the anode.

Evidently, different carbon materials, for instance natural and synthetic graphite, show different behavior during lithiation at normal temperatures,<sup>17</sup> and the nature of the solvent and its composition also play a role.<sup>18</sup> From existing literature data, there is an indication that temperature deteriorates the capacity of Li/C electrodes,<sup>10–16</sup> however, the amount of the experimental material is unsatisfactory to make general conclusions on the mechanism of the influence of temperature in a particular system. It is to be expected that different carbon materials may respond in different manners to lithiation at elevated temperatures, even in an electrolyte of the same composition. In this sense, in this work, both the irreversible capacity and the impedance parameters of a synthetic graphite of the trademark KS44 (Lonza), lithiated initially in a solution EC+PC (1:1) + 1 M LiClO<sub>4</sub>, either at room temperature at low charging rate or at elevated temperature at a higher charging rate, were studied. This material is otherwise known to have low irreversible capacity at room temperature in PC containing electrolytes.<sup>17</sup>

#### EXPERIMENTAL

The electrochemical intercalation/deintercalation of the synthetic graphite KS44 (Timcal AG, Sins, Switzerland, former Lonza), was carried out using a two-electrode cell (Fig. 1). The cell consisted of a porous graphite electrode supported by a copper foil (with a geometric area of 5 cm<sup>2</sup>, and a weight of 1.83 mg/cm<sup>2</sup> graphite), and a lithium foil (Lithium Corporation of America) as both the counter and reference electrode. According to the manufacturer, the graphite average grain size was 44 μm, and the BET surface area amounted to 10 m<sup>2</sup> g<sup>-1</sup>.

Graphite electrodes were made by mixing a slurry containing 6 wt % poly(vinylidene fluoride) binder (Aldrich) and 94 wt. % graphite powder in a *N*-methyl-2-pyrrolidinone solution (Aldrich). The slurry was applied on a copper foil current collector. The wet deposits was then dried in a vacuum-oven at 120 °C for 2 h.

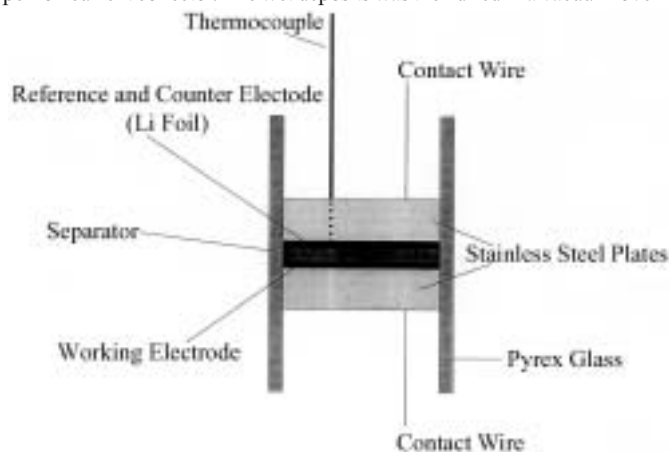


Fig. 1. The cell configuration.

A filter paper, serving simultaneously as a separator and electrolyte carrier, was soaked with the electrolyte, composed of 1 M LiClO<sub>4</sub> (Lithium Corporation of America) in a solvents mixture ethylene carbonate (Fluka)/propylene carbonate (Fluka) (1 M:1 M).

The working and counter electrodes were permanently sandwiched together.

The cells were assembled in a glove box, in which the moisture level was less than 20 ppm.

The electrochemical measurements, involving both galvanostatic charge-discharge and AC impedance measurements, were carried out using a EG&G Princeton Applied Research Galvanostat/Potentiostat, Model 273, coupled with an EG&G Princeton Applied Research Two Phase Lock-in Analyzer, Model 5208.

## RESULTS AND DISCUSSION

The first galvanostatic lithiation/delithiation cycle of synthetic graphite KS44, in solution PC+EC (1 M:1 M) + 1 M LiClO<sub>4</sub> are shown in Fig. 2a and b. The upper Figure a relates to lithiation (charging) at room temperature with a current density of 10  $\mu\text{A mg}^{-1}$ , and the bottom Figure b relates to lithiation at the elevated temperature of 55  $^{\circ}\text{C}$  with a current density of 30  $\mu\text{A mg}^{-1}$ . In both cases, discharging was carried out under the same conditions, *i.e.*, at room temperature using a current density of 20  $\mu\text{A mg}^{-1}$ .

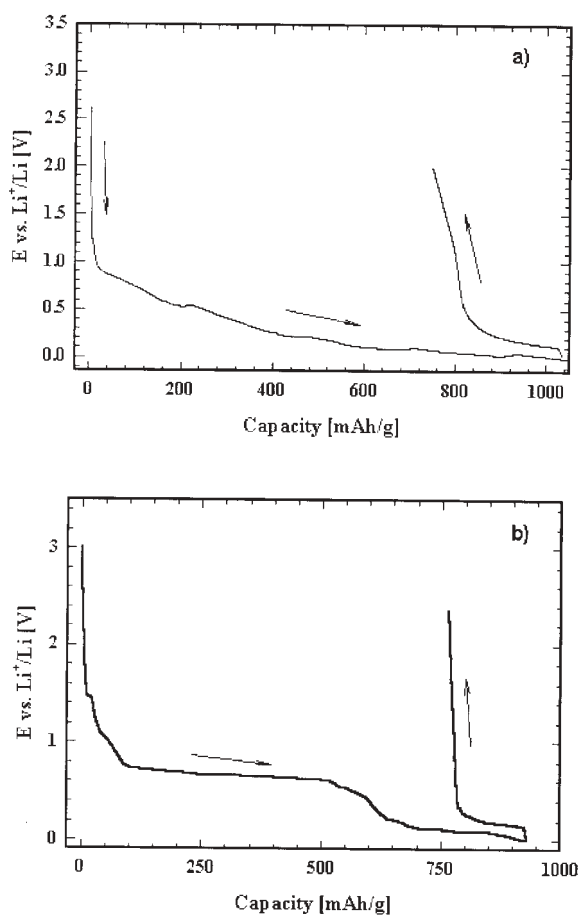


Fig. 2. Initial charge and discharge curves of synthetic graphite Lonza KS44 in 1 M LiClO<sub>4</sub>/EC + PC (1 M:1 M): (a) charge current density: 10  $\mu\text{A mg}^{-1}$ , discharge current density: 20  $\mu\text{A mg}^{-1}$ , room temperature; (b) charge current density: 30  $\mu\text{A mg}^{-1}$ , temperature: 55  $^{\circ}\text{C}$ ; discharge current density: 20  $\mu\text{A mg}^{-1}$ , room temperature.

Different charging rates were used at different temperatures, because the graphite charging rate is limited by the rate of lithium diffusion through the graphite. Namely, the charging rate must be slow enough to prevent the appearance of cathodically deposited lithium in the metallic form on the graphite/electrolyte interface. In this work, for the first room temperature charging, a rate of  $10 \mu\text{A mg}^{-1}$  was used which is a middle value between the  $5$  and  $20 \mu\text{A mg}^{-1}$  used by Wang *et al.*<sup>15</sup> and by Guerin *et al.*,<sup>17</sup> respectively. In choosing the charging rate at elevated temperature, it must be remembered that the solids are known to possess a high activation energy of diffusion, and that temperature elevation causes an abrupt increase in the rate of diffusion. Therefore, it is to be expected that charging rate may be allowed at elevated temperatures. However, in our case, the higher charging rate was found to be not only allowed, but also necessary. In preliminary experiments at  $55^\circ\text{C}$ , we evidenced that at charging rates of  $10$  and  $20 \mu\text{A mg}^{-1}$ , all the charge was consumed by processes occurring at approx.  $1 \text{ V}$ , *i.e.*, no SEI formation was observed, even if the charge consumed was several times greater than the amount required for SEI formation at room temperature. A charging rate of  $30 \mu\text{A mg}^{-1}$ , however, resulted in the appearance of a SEI which in the voltage–time profiles, was reflected by a further potential drop to nearly  $0 \text{ V}$ . Probably at this elevated temperature one is dealing with a competition between the dissolution of the reduction products, and their precipitation within the graphite particles in the form of an SEI. Therefore, there is not only an upper limiting value of the charging rate, but also a lower limiting one. In our experiments a charging rate of  $30 \mu\text{A mg}^{-1}$  was used. However, it should be noted that this charging rate is not necessarily the one which leads to the minimum irreversible capacity at this temperature.

As is obvious from Figs. 2a and 2b, in the early stage of charging at both temperatures, the potential dropped rapidly from the open circuit value of approx.  $3 \text{ V}$ , to *ca.*  $1.0 \text{ V}$ . For the electrode lithiated at room temperature with a current density of  $10 \mu\text{A mg}^{-1}$ , after reaching *ca.*  $1 \text{ V}$ , a short shoulder was registered, but the potential continued to decrease monotonously. The appearance of the shoulder means a decomposition of the solution which leads to electrode passivation due to the formation of a SEI. This should result in a reduction of current losses caused by electrolyte decomposition in further lithiation/delithiation cycles. For the electrode charged at the elevated temperature with a charging rate of  $30 \mu\text{A mg}^{-1}$ , upon reaching *ca.*  $1 \text{ V}$ , the potential remained nearly constant till a capacity of  $540 \text{ mAh g}^{-1}$  was achieved, then it dropped suddenly to *ca.*  $0 \text{ V}$  and remained almost constant at this value from  $620 \text{ mA/h g}^{-1}$  up to  $940 \text{ mAh g}^{-1}$ . From the slow cyclic voltammetric measurement by Aurbach *et al.*,<sup>19</sup> it is known that graphite lithiation takes place at the potentials below  $0.3 \text{ V vs Li/Li}^+$ . The potential plateau in the capacity range  $0$  to  $540 \text{ mAh g}^{-1}$  means that this process corresponds not to lithiation but to other processes, such as solvent decomposition accompanied by graphite rupture (exfoliation), as was shown elsewhere in other systems.<sup>1,9,19</sup> Therefore, in the system under investigation, a temperature elevation of only  $30^\circ\text{C}$  appeared to be large enough to cause a considerable irreversible loss of capacity, caused by graphite exfoliation. This reduces the amount of electrode material available to further cycling, which is visible already during the following delithiation (Fig. 2b, discharge curve).

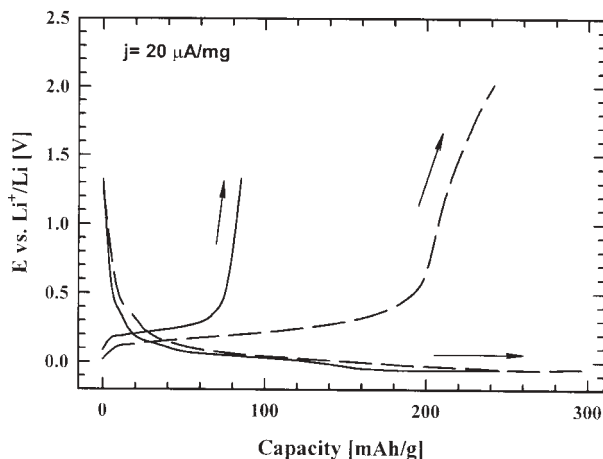


Fig. 3. Second, room temperature, charge/discharge curves for synthetic graphite KS44 in 1 M LiClO<sub>4</sub>/EC+PC (1 M:1 M) lithiated at room temperature (dashed line) and at 55 °C (full line), at a common current density of 20 μA mg<sup>-1</sup>.

The two cells, the first charging/discharging voltage–time profiles of which were presented in Fig. 2, were exposed to a further second galvanostatic charge/discharge cycle, in both cases performed at room temperature and at a rate of 20 μA mg<sup>-1</sup>. The resulting voltage–time profiles are presented in Fig. 3. The discrepancy of the achieved discharging capacities of the electrodes within the two cells is very pronounced. The electrode charged initially at room temperature showed a discharging capacity which was almost four times higher than the one initially charged at 55 °C. That means that the SEI layer formed at the elevated temperature, although much thicker, protects the electrolyte from further reduction much less effectively than that formed at room temperature.

A further room-temperature cycling of the electrode charged initially at room temperature was carried out with a current density of 20 μA mg<sup>-1</sup>. This experiment evidenced that, in the several following cycles, the electrode displayed an additional irreversible capacity loss, but in the fourth and the fifth cycle convergence was reached, and in subsequent cycles the discharging capacity became constant. Contrary to this, the electrode initially charged at 55 °C did not display this convergence in the fifth cycle.

The fifth galvanostatic charging and discharging curves of the electrode formed at room temperature and, for the sake of comparison, the second galvanostatic charging and discharging curve of the electrode charged initially at elevated temperature are presented in Fig. 4a. There is obviously a significant difference between their discharge capacities, in favor of the electrode charged initially at room temperature. Namely, the electrode charged initially at room temperature, after even five charge/discharge cycles, displayed more than two times higher discharging capacity than the electrode charged initially at 55 °C during its second discharging.

An electrode which had initially been charged at room temperature, and had undergone a further four room temperature charging/discharging cycles with 20 μA mg<sup>-1</sup> (the last of which is illustrated in Fig. 4a), was subjected to further treatment in the following way: it was heated up to 55 °C, and cycled additionally five times with a current density of 30 μA mg<sup>-1</sup>. Exceptionally, the last of the ten discharging of this electrode was carried out

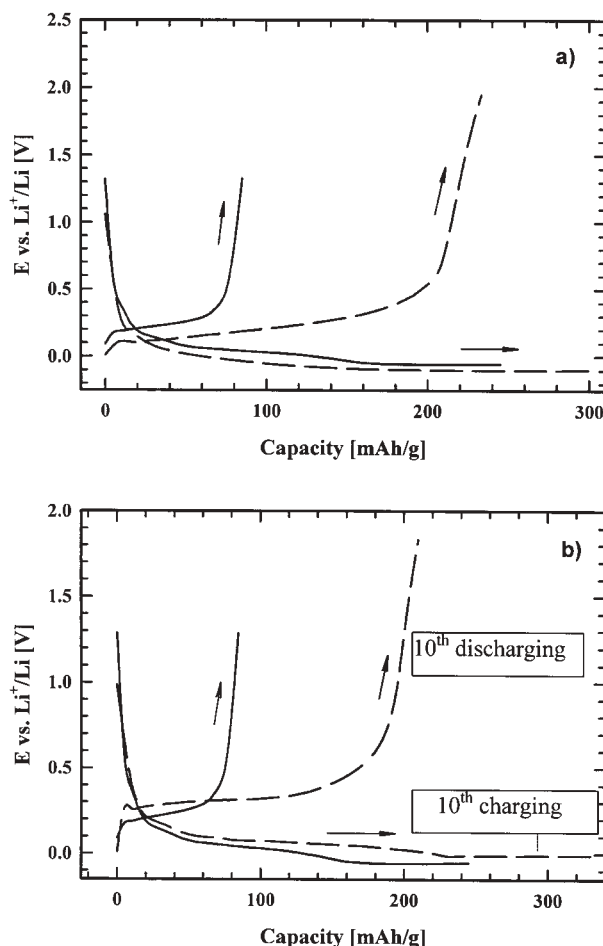


Fig. 4. Charging/discharging curves for synthetic graphite KS44 in 1 M  $\text{LiClO}_4$ /EC+PC (1 M:1 M): (a) (- - -): fifth charging and discharging curve for an electrode lithiated initially at room temperature with a current density  $10 \mu\text{A mg}^{-1}$ , and cycled a further four times at room temperature with a current density of  $20 \mu\text{A mg}^{-1}$ ; (—): second, room temperature, charging and discharging curve for an electrode lithiated initially at  $55^\circ\text{C}$  (copied from Fig. 3); (b) (- - -): 10th charging and discharging curve for an electrode lithiated initially at room temperature, then cycled four times at room temperature with a current density of  $20 \mu\text{A mg}^{-1}$ , then heated to  $55^\circ\text{C}$  and cycled a further five times with current density  $30 \mu\text{A mg}^{-1}$ , but only in the last, tenth cycle, was the discharging carried out at room temperature with a current density of  $20 \mu\text{A mg}^{-1}$ ; (—): second charging and discharging curve for an electrode lithiated at  $55^\circ\text{C}$  (copied from Fig. 3).

at room temperature with a current density of  $20 \mu\text{A mg}^{-1}$ . The tenth charging and discharging curves of this electrode are presented in Fig. 4b. For the sake of comparison, the second charging and discharging curve of the electrode charged initially at  $55^\circ\text{C}$ , already presented in Fig. 4a, is also presented in Fig. 4b. It is obvious that the electrode charged initially at room temperature, after this tenfold cycling at both room and elevated temperature, retained a more than two times higher reversible capacity than the one charged initially at  $55^\circ\text{C}$  in its next charge/discharge cycle. This illustrates that the initial charging conditions play a crucial role in the formation of a well protecting SEI layer.

The impedance measurements were performed before and after the first galvanostatic charging and discharging, and the results are given, for the electrode charged at room temperature in Fig. 5 and, for that charged at  $55^\circ\text{C}$  in Fig. 6. Additionally, in Fig. 5, the room temperature impedance diagram of a graphite electrode recorded before intercalation, at its open circuit potential, is presented.

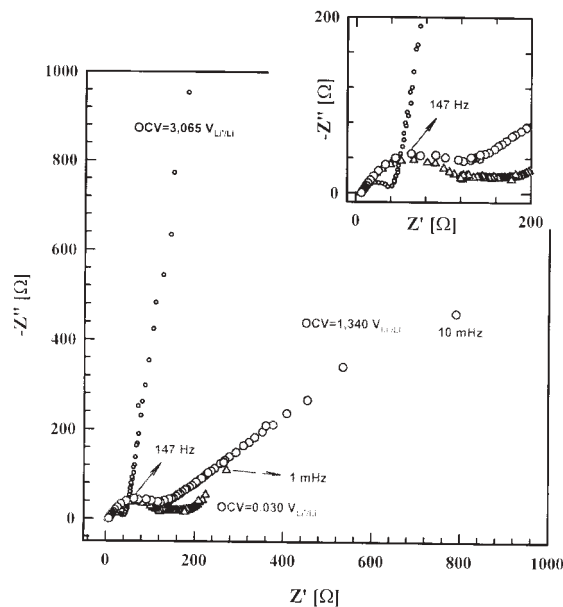


Fig. 5. Impedance diagrams of graphite KS44 before intercalation (●), after intercalation up to  $\text{LiC}_6$  composition ( $\Delta$ ) and after discharge (○), all recorded at room temperature and at their own open circuit potentials (OCV). Open circuit potentials vs.  $\text{Li/Li}^+$  (OCV) are indicated in each diagram.

The interfacial impedance data may be interpreted by means of the equivalent circuit given in Fig. 7. The equivalent circuit is a reduced form of the circuit used by Wang *et al.*<sup>15</sup>

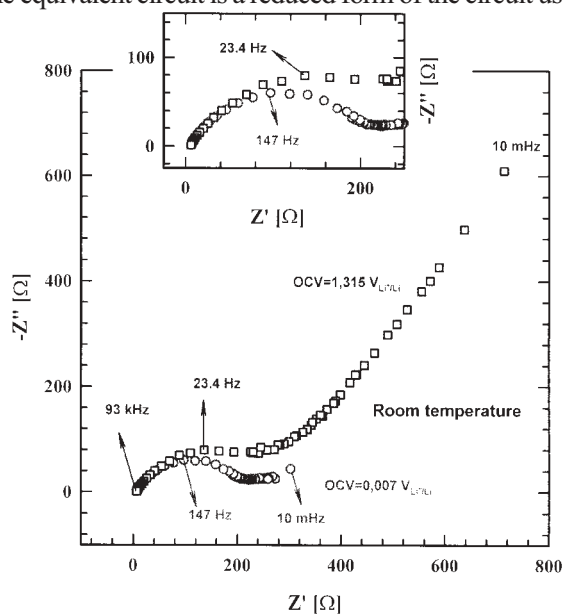


Fig. 6. Impedance diagrams of a Li/C electrode recorded at room temperature after charging up to  $\text{LiC}_6$  composition at  $55^\circ\text{C}$  (○), and after discharging at room temperature (□).

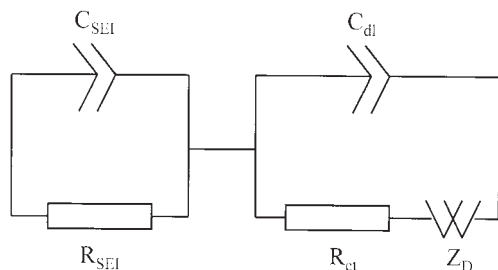


Fig. 7. Equivalent circuit used to simulate the impedance diagrams.  $C_{SEI}$  and  $C_{dl}$  are SEI capacitance and SEI/graphite double layer capacitance, respectively,  $R_{SEI}$ ,  $R_{ct}$  are SEI resistance and charge transfer resistance of the redox reaction  $Li^+ + e^- = Li$ , respectively,  $Z_D$  is the diffusion impedance.

Namely a thin layer of copper supported anode material was used, which displays less impedance elements than does a pellet of carbon powder pressed between the two nickel meshes in Ref. 15, and, therefore, a SEI multilayer model was unnecessary. It consists of a SEI impedance and a graphite/SEI double layer impedance in a series connection. To this circuit a liquid solution resistance should be added, however this was negligible in our measurements. Since the impedance semicircles were distorted, the capacitances are used as distributed elements (so called constant phase elements, CPE) of the form:

$$C_1 = C\omega^n - [\cos(n\pi/2 + i \sin(n\pi/2)]$$

with  $n = 0.8$ . The diffusion impedance  $Z_D$  has the form:

$$Z_D = (1 - i) \sigma \omega^{-m}$$

where  $m$  is close to 0.5, and in the case when  $m = 0.5$  one is dealing with a regular Warburg impedance. The diffusion constant  $\sigma$  for lithiation/delithiation has a particular form derived by Ho *et al.*<sup>20</sup>

$$\sigma = V_m(dE/dx)/FA(2D)^{1/2}$$

where  $V_m$  is the molar volume of the lithiated material,  $dE/dx$  is the slope of the dependence of the open circuit potential ( $E$ ) versus the level of charge ( $x$ ) (assuming the formula  $Li_xC_6$  for lithiated carbon),  $A$  is the electrochemically active area, and  $D$  is the chemical diffusion coefficient of lithium. As with classical Warburg diffusion, the diffusion constant is inversely proportional to the concentration of the diffusing species. The impedance diagrams in Fig. 8, calculated on the basis of this equivalent circuit for the frequency range 10 mHz to 100 kHz, correspond well to the experimentally determined diagrams given in Figs. 5 and 6.

The impedance diagram of a graphite electrode before lithiation, recorded at its open circuit potential of 3.065 V (shown in Fig. 5), appears to be relatively simple, consisting of a high-frequency semicircle and a low frequency straight line vertical to the real axis, which is characteristic of an almost purely capacitive impedance. We interpret this equivalent circuit as metal/graphite particle contact impedance (consisting of a contact resistance and contact capacitance in parallel) connected serially to a double layer capacitance. This equivalent circuit is quite similar to that proposed by Chang and Sohn<sup>21</sup> for Osaka Gas graphitised mesocarbon microbeads dispersed on a copper foil, and corresponds generally to a metal/electrolyte boundary in the absence of a redox pair.

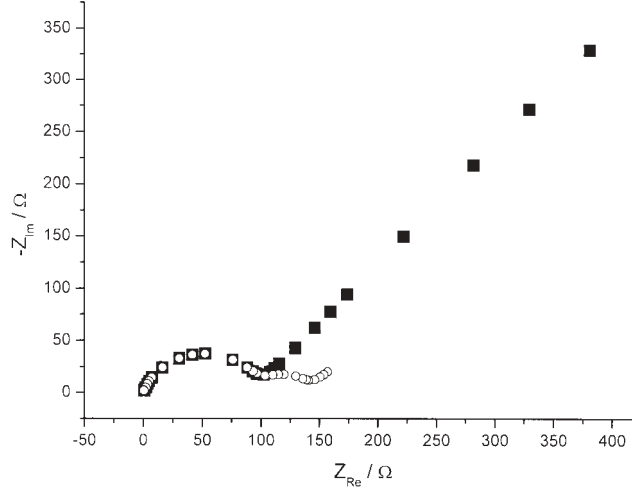


Fig. 8. Impedance diagrams calculated in the frequency range 10 mHz to 100 kHz, on the basis of the equivalent circuit presented in Fig. 7 with  $C_{SEI} = 0.00005 * \omega^{0.8} [\cos(0.8\pi/2) + i \sin(0.8\pi/2)]$ ,  $C_{dl} = 0.005 * \omega^{0.8} [\cos(0.8\pi/2) + i \sin(0.8\pi/2)]$ ,  $R_{SEI} = 100$  ohm,  $R_{ct} = 40$  ohm,  $\sigma = 100$  ohm  $s^{1/2}$  (solid squares) and  $\sigma = 5$  ohm  $s^{1/2}$  (open circles).

After the graphite had been lithiated up to a potential of 0.0 V vs. Li/Li<sup>+</sup>, the impedance diagram transformed into a series of two semicircles, a high and a low frequency one. The manner of their change with changing degree of charging, discussed below, enable the conclusion that the high-frequency one is due to the resistance of the SEI and the low-frequency one is due to the resistance of the lithium redox reaction. The radius of the high frequency semicircle presents the resistance of the SEI formed around the lithiated graphite particles. Probably, this resistance also involves the interparticle contact resistance, however, either due to the predominance of one of them, or due to the overlapping of the corresponding time constants, only one impedance semicircle corresponding to the solid electrolyte appears. The low frequency semicircle is assigned to the resistance of the lithium redox reaction at the lithiated graphite/SEI interface. It is obvious that the sample lithiated at room temperature shows lower resistance parameters than the one lithiated at the elevated temperature, which is a consequence of the SEI formed at room temperature being thinner (Table I).

TABLE I. Room temperature values of the resistance parameters of the lithiated and delithiated graphite corresponding to the impedance diagrams in Figs. 5. and 6, for sample initially lithiated at 25 °C and 55 °C

	25 °C		55 °C	
	Lithiated	Delithiated	Lithiated	Delithiated
$R_{SEI}/\text{ohm}$	122	150	220	260
$R_{ct}/\text{ohm}$	60	*	70	*
$\sigma/\text{ohm s}^{1/2}$	7.9	110	10	150

\* $R_{ct}$  determination for the delithiated samples is inaccurate due to a considerable overlapping of the charge transfer and diffusion impedance

In Fig. 5, the points corresponding to extremely low frequencies lie on a straight line. This part of the impedance diagram may be interpreted as a mass transfer impedance of lithium through the graphite particles.<sup>15,21–23</sup> For fully lithiated graphite, down to a frequency of 10 mHz, the mass transfer limitations appear to be practically absent, which is due to the obviously high concentration of intercalated lithium. However, the samples discharged to an open circuit potential of 1.3 V, display a considerable mass transfer impedance of nearly Warburg type.

It is worth mentioning that in the system under investigation, the radius of the high-frequency semicircle, attributed to the SEI resistance, only slightly increases when the lithiated sample is fully delithiated, while simultaneously, the diffusion constant increases by a whole order of magnitude (Table I). This means that delithiation does not change the conductivity of the SEI, connected to the concentration and mobility of  $\text{Li}^+$  ions within the SEI. This, in turn, evidences that indeed one should attribute the low frequency parts of impedance diagrams exclusively to diffusion processes within the graphite and not to diffusion through the SEI. This is an important conclusion, since in the literature there exists a permanent uncertainty relating to the correctness of the assignment of the impedance semicircles of lithiated carbon electrodes. For instance, a very extensive investigation was performed recently by Wang *et al.*<sup>15</sup> in order to contribute to this topic, and our assignment is in accordance with this work.

*Acknowledgement:* The first three authors are grateful to the Ministry of Science, Technology and Development of the Republic of Serbia, for supporting this work through the contract entitled “Structure, thermodynamic and electrochemical properties of modern materials relevant for energy conversion and components in electronics”.

#### ИЗВОД

### УТИЦАЈ ТЕМПЕРАТУРЕ НА ИНТЕРКАЛАЦИЈУ ЛИТИЈУМА У ГРАФИТ KS44 У РАСТВОРУ ЕТИЛЕН КАРБОНАТ + ПРОПИЛЕН КАРБОНАТ: ИСПИТИВАЊЕ ГАЛВАНОВАТНОМ И ИМПЕДАНСНОМ МЕТОДОМ

Б. БЛИЗАНАЦ<sup>1</sup>, С. МЕНТУС<sup>1</sup>, Н. ЦВЈЕТИЋАНИН<sup>1</sup> И Н. ПАВЛОВИЋ<sup>2</sup>

<sup>1</sup>Факултет за физичку хемију, Студентски брз 12–16, Београд и <sup>2</sup>Војно-технички институт Војске Југославије, Капанићева 15, Београд

Графит Lonza KS44 био је галваностатски интеркалиран и деинтеркалиран литијумом у раствору 1 M  $\text{LiClO}_4$  у еквимоларној смеси етилен карбоната и пропилен карбоната, на собној температури и на повишеној температури од 55 °C. За овај специфичан систем снимана је зависност потенцијала од времена, а за интеркалиране и деинтеркалиране узорке снимљени су импедансни дијаграми. Потврђено је да литијација на собној температури не производи знатне губитке струје везане за редукцију молекула електролита између графитних равни. Међутим, за интеркалацију на повишеној температури карактеристична је појава напонског платоа који у јединицама електродног капацитета траје 540 mAh, и овај део ирверзибилног капацитета је последица раслојавања графитних равни (ексфолијације). Слој чврстог електролита око честица графита који се формира приликом интеркалације литијума на повишеној температури, иако лошије спречава даљу редукцију електролита, показује двоструко већи електрични отпор од слоја који се формира на собној температури. Упоредивање

импедансних дијаграма интеркалираног и деинтеркалираног узорка води закључку да је за дифузионе процесе из нискофреквентних области импедансних дијаграма одговорна искључиво дифузија кроз графит а не и кроз слој чврстог електролита.

(Примљено 18. августа, ревидирано 23. октобра 2002)

## REFERENCES

1. M. Winter, J. O. Besenhard, M. E. Spahr, P. Novak, *Adv. Mater* **10** (1998) 725
2. J. O. Besenhard, H. P. Fritz, *J. Electroanal. Chem.* **53** (1974) 329
3. J. O. Besenhard, M. Winter, J. Yang, W. Biberacher, *7<sup>th</sup> Int. Meeting on Lithium Batteries*, Extended Abstracts, p. 278, Boston, 1994
4. J. O. Besenhard, M. Winter, J. Yang, W. Biberacher, *J. Power Sources* **54** (1995) 228
5. D. Aurbach, Y. Ein-Eli, O. Chusid, Y. Carmeli, M. Babai, H. Yamin, *J. Electrochem. Soc.* **141** (1994) 603
6. R. Fong, U. von Sacken, J. R. Dahn, *J. Electrochem. Soc.* **187** (1995) 999
7. S. Mori, H. Asahina, H. Suzuki, A. Yonei, E. Yasukawa, *8<sup>th</sup> International Meeting on Lithium Batteries*, Extended Abstracts, p. 40, Nagoya, 1996
8. M. Inaba, Z. Siroma, A. Funabiki, Z. Ogumi, *Langmuir* **12** (1996) 1535
9. M. Ihaba, Z. Siroma, Y. Kawadate, A. Funabiki, Z. Ogumi, *8<sup>th</sup> International Meeting on Lithium Batteries*, Extended Abstracts, p. 181, Nagoya, 1996
10. A. M. Anderson, K. Edstrom, N. Rao, A. Wendsjo, *J. Power Sources* **81–82** (1999) 286
11. A. M. Anderson, K. Edstrom, J. O. Thomas, *J. Power Sources* **81–82** (1999) 8
12. D. D. MacNeil, D. Larcher, J. R. Dahn, *J. Electrochem. Soc.* **146** (1999) 3596
13. T. Zheng, A. S. Gozdz, G. G. Amatucci, *J. Electrochem. Soc.* **146** (1999) 4014
14. A. M. Anderson, M. Hersted, A. G. Bishop, K. Edstrom, *Electrochim. Acta* **47** (2002) 1885
15. C. Wang, A. J. Apleby, F. Little, *Electrochim. Acta* **46** (2001) 1793
16. D. Aurbach, B. Markowsky, A. Rodkin, M. Cojocar, E. Levi, Hzeong-Jin Kim, *Electrochim. Acta* **47** (2002) 1899
17. K. Guerin, A. Fevrier-Bouvier, S. Flandrois, M. Couzi, B. Simon, P. Biensan, *J. Electrochem. Soc.* **146** (1999) 3660
18. M. C. Smart, B. V. Ratnakumar, S. Surampudi, Y. Wang, X. Zhang, S. G. Greenbaum, A. Hightower, C. C. Ahn, B. Fultz, *J. Electrochem. Soc.* **146** (1999) 3963
19. D. Aurbach, B. Markowsky, I. Weissman, E. Levi, Y. Ein-Eli, *Electrochim. Acta* **45** (1999) 67
20. C. Ho, I. D. Raistrick, R. A. Huggins, *J. Electrochem. Soc.* **127** (1980) 343
21. Y.-C. Chang, H.-J. Sohn, *J. Electrochem. Soc.* **147** (2000) 50
22. D. Aurbach, M. D. Levi, E. Levi, H. Teller, B. Markowsky, G. Salitra, U. Heider, L. Heider, *J. Electrochem. Soc.* **145** (1998) 3024
23. P. Yu, B. N. Popov, J. A. Ritter, R. E. White, *J. Electrochem. Soc.* **146** (1999) 8.